

# Singularities of the interaction of laser radiation with materials at high pressure of the surrounding medium

N. N. Rykalin, A. A. Uglov, and M. M. Nizametdinov

*Baïkov Metallurgy Institute, USSR Academy of Sciences*

(Submitted March 13, 1975)

Zh. Eksp. Teor. Fiz. 69, 722–732 (August 1975)

Experimental data are presented on the interaction of the radiation of a neodymium laser with materials (metals or dielectrics) at high pressure of the surrounding medium. It is shown that an increase of the ambient pressure in the range 30–100 atm at a flux density  $10^6$ – $10^7$  W/cm<sup>2</sup> leads to almost complete screening of the target by a plasma cloud. The primary mechanism whereby a zone of laser-radiation absorption is produced in a cold gas at high pressure near the target is the thermionic emission (at weak evaporation) and breakdown in the evaporated matter (in the case of developed evaporation). The main mechanism that maintains the plasma cloud at flux densities 1–10 MW/cm<sup>2</sup> is the slow combustion. It is noted that periodic variation of the plasma brightness after the termination of the action of the radiation on the dielectrics can be attributed to release of the energy of the chemical reaction, the development of which is determined by the time required to attain the temperature, which itself depends on the particle dimensions. The characteristics of the target in the interaction zone, which depend on the radiation flux density and on the gas pressure in the chamber, are considered.

PACS numbers: 79.20.Ds, 42.60.Nj

## 1. INTRODUCTION

The action of pulsed and continuous laser radiation on targets made of materials having different physical properties and under high pressure has not been studied sufficiently. The published systematic experimental data pertain to the breakdown of cold gases at high pressures up to  $\sim 2000$  atm by single-pulse radiation at radiation flux densities  $q$  exceeding  $10^9$  W/cm<sup>2</sup> (see the review<sup>[1]</sup>) but in the absence of a solid target.

It is known that if the gas pressure in the chamber is on the order of several dozen atmosphere it is possible to maintain their a stationary optical discharge ("laser plasmotron") with the aid of continuous or pulsed radiation, if breakdown of the gas has been effected beforehand, i.e., if a "priming" plasma has been produced by pulsed radiation with a flux density exceeding  $\sim 10^9$  W/cm<sup>2</sup><sup>[2]</sup> or by some other method. If a solid target is placed near the focus of the optical system, then the breakdown-development threshold is reduced for both millisecond and nanosecond radiation. This fact was noted, for example, in studies by Bonch-Bruевич et al.,<sup>[3]</sup> where placing a mirror transparent to the radiation near the focus of the lens lowered the breakdown threshold of air at atmospheric pressure by a factor 2–5 for a monopulse of 50 nsec duration and for a radiation flux density  $q \sim 10^{10}$  W/cm<sup>2</sup>.

According to the data of Barchukov et al.,<sup>[4,5]</sup> low-pressure breakdown of gas by CO<sub>2</sub> laser radiation (wavelength  $10.6 \mu$ ) is due to breakdown of matter evaporated from the surface of the metallic or dielectric target (impurity dielectric layer). It is noted, however, that polishing the metal target raises the threshold of the developed evaporation and the low-threshold gas breakdown cannot be due to evaporation of the metal. Depending on the radiation flux density, two essentially different plasma-motion regimes are realized—that of optical detonation and that of the "laser plasmotron."<sup>[4]</sup>

Goncharov et al.<sup>[6]</sup> obtained breakdown in evaporated metal at atmospheric pressure in air and at flux densities  $q \sim 2 \times 10^7$  W/cm<sup>2</sup> in the focus of a lens placed  $\approx 10$  mm away from the target surface (flux density at the target  $\sim 2 \times 10^6$  W/cm<sup>2</sup>).

The main purpose of the cited studies<sup>[1-6]</sup> was to investigate the conditions of gas breakdown and the characteristics of the resultant discharges (temperature, absorption coefficient, propagation velocity, etc.) At the same time, the changes of the physical characteristics of the targets under these conditions have not been investigated to any degree. Our earlier papers<sup>[7,8]</sup> cite experimental data on gas breakdown near the surface of a metallic target at high ambient pressures in the flux density range  $\sim 10^6$ – $10^7$  W/cm<sup>2</sup> and report production of a long-lived (compared with the pulse duration) plasma that screens the target from the direct action of neodymium-laser radiation.

In this paper we study the development of a plasma cloud near a target in nitrogen, discuss the discharge propagation mechanism, and consider the changes in the physical characteristics of targets acted upon by radiation.

## 2. EXPERIMENTAL DATA

The setup for experiments on the action of radiation on a target in a controlled medium with variable pressure is described in<sup>[7]</sup>. We used in the experiments a neodymium laser with pulse duration  $\tau_p \sim 0.8$  msec; the pulse energy ranged from several joules to several dozen joules; the focal length of the lens was 150 mm; the flux density ranged from  $\sim 10^6$  to  $10^7$  W/cm<sup>2</sup> at a heating-spot radius 0.03–0.05 cm. The radiation pulse had a spike structure with characteristic spike duration  $\sim 1 \mu$ sec. The targets were plates of metal (molybdenum, stainless steel) 1–2 mm thick and dielectric plates (22Kh high-temperature ceramic, bakelite). The pressure of the gas (nitrogen) in the chamber was varied between 1 and 140 atm.

At high pressures, the action of the laser radiation on the material leads to screening of the action zone and to a change in the character of the damage to the target.<sup>[7,8]</sup> We consider separately the experimental data on the phenomena that occur over the surface of the target, and the changes produced by the joint action of the radiation and the high pressure in the physical characteristics of the targets.

a) Development of screening zone, evolution of plasmoid. A study of the kinetics of the development of the plasma cloud was carried by high speed photography with the SFR-1 camera operating in the time-magnifier mode. The time interval between individual frames ranged from 15 to 80  $\mu\text{sec}$ , depending on the degree of detail in which the particular stage of the process was investigated.

The experimental data show that  $\sim 30\text{--}50 \mu\text{sec}$  after the start of the action of the radiation, at a gas pressure of several dozen atmospheres and a flux density  $q \sim 10^6\text{--}10^7 \text{ W/cm}^2$ , a plasma cloud develops above the surface of the target and screens the action zone almost completely against the direct incidence of radiation. The degree of screening of the target by the plasma cloud, which is determined by the mass of the removed matter, depends essentially on the variation of the pressure and less strongly on the flux density. The plasma cloud is produced near the target surface and moves opposite to the laser beam at a velocity 2–5 m/sec at flux densities  $q \sim 10^6\text{--}10^7 \text{ W/cm}^2$ .

Figure 1 shows the experimental data on the change of the speed of the plasma cloud when radiation acts on a stainless-steel plate in a nitrogen atmosphere. We see that the speed reaches a maximum value  $\approx 5 \text{ m/sec}$  at the end of the pulse and then begins to decrease. The lifetime of the plasma cloud is almost double the pulse duration ( $\tau_p = 0.8 \text{ msec}$ ) for such materials as molybdenum and stainless steel. The plasma cloud produced by the action of the radiation on dielectrics (22Kh ceramic, bakelite) has a longer lifetime, about 4 msec.

Figure 2 shows data on the lifetime of the plasma cloud for various materials. Attention is called to the rather long lifetime of the plasma prior to its recombination, for such materials as bakelite ( $\sim 4.5 \text{ msec}$  at a laser pulse duration 0.8 msec). An interesting feature is also the fact that the plasmoid temperature seems to increase after the end of the pulse, since the brightness of the plasma increases at the time  $\approx 2 \text{ msec}$ . The situation is similar for the 22Kh ceramic, except that these phenomena are less clearly pronounced.

The transverse dimension of the plasmoid for metallic targets changes with time, first increasing and then decreasing to a definite value that depends on the gas pressure and on the radiation flux density, changing little up to the instant when the cloud disappears (Fig. 3). The latter seems to indicate that the pressure in the plasmoid at the end of the pulse differs little from the pressure of the gas in the chamber.

The change of the transverse dimension of the plasma cloud for a number of dielectric materials, as a function of the gas pressure and the radiation flux density, is shown in Fig. 4. It is seen that for dielectrics the pressure in the plasma is almost always different from the pressure of the gas in the chamber for the given range of variation of the parameters.

In all the investigated materials, the plasma cloud was produced near the target surface. It turned out to be difficult to determine the distance from the breakdown region to the target at the geometry used in the experiments for the photography of the interaction zone, inasmuch as the process was photographed at right angle to the laser beam. We note that in a number of experiments the target density was not at right angle to the laser beam direction. This did not influence the development of the

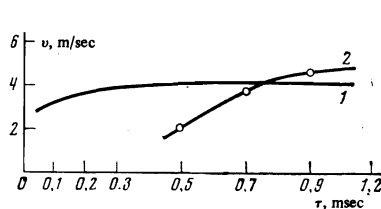


FIG. 1

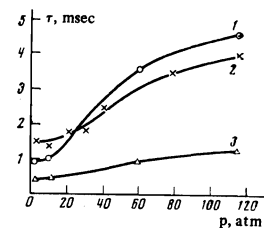


FIG. 2

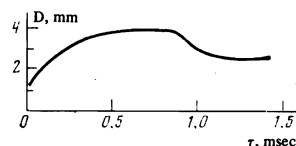


FIG. 3

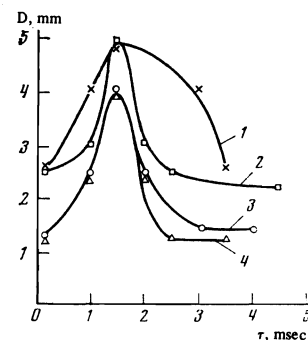


FIG. 4

FIG. 1. Change in the velocity of the plasmoid with time, in the case of stainless steel: 1—calculated curve, 2—experimental data.  $p_0 = 70 \text{ atm}$ ,  $q = 10^7 \text{ W/cm}^2$ .

FIG. 2. Lifetime of plasma cloud for a number of materials: 1—bakelite, 2—ceramic, 3—stainless steel.

FIG. 3. Change of transverse dimension of plasmoid with time in the case of metals.

FIG. 4. Change of transverse dimension of plasmoid with time for dielectrics. Bakelite: 1—at  $p = 60 \text{ atm}$ , 2— $p = 120 \text{ atm}$ ; ceramic: 3— $p = 120 \text{ atm}$ , 4— $p = 60 \text{ atm}$ .

target screening, inasmuch as when the plane of the target was rotated the plasma cloud moved in a direction opposite to the target beam, and not normal to the target. This agrees with the published reports that the breakdown zone moves along the laser beam in experiments with lower pressures. [5, 9]

The optical density of the plasma cloud is not uniform. At the center of the plasmoid the pressure is higher, and the outer boundary is diffuse. The plasmoid radiation brightness varies with time. This is particularly strongly pronounced for bakelite, the increase of the plasmoid brightness being observed without the light energy flowing into the volume of the plasma. This may be due, in our opinion, to the combustion of the minute particles of the bakelite or the ceramic, which are ejected from the disintegration zone (the pertinent estimates will be given later on), the heating time of which in the plasma (to a temperature above their "ignition point") exceeds the radiation-pulse duration.

b) Change of the target parameters in the laser-radiation action zone. Independently of the target material (metal or dielectric), screening by the plasmoid decreases strongly the outflow of the material. At a target thickness 1–2 mm and an ambient pressure up to 20–30 atm (flux density  $q \sim 10^6\text{--}10^7 \text{ W/cm}^2$ ), a hole is cut through the target, and the fraction of the molten material on the target surface is small. An increase of the pressure (at the indicated flux densities) leads to almost complete screening of the radiation when the target surface is merely "scorched" (covered with a thin layer of oxides) and has practically no microscopic regions with minute droplets of the melt. At the same time, the dimensions of the zone of action of the laser

radiation on the target increase appreciably: at an initial dimension of the heating spot  $r_f \approx 0.025-0.03$  cm, the dimensions of the scorched zone amount to several tenths of a millimeter, i.e., the increase severalfold.

It is natural to relate this fact to the change in the spatial and temporal characteristics of the heat source acting on the surface of the target after the start of the development of the screening. The flux density of the heat source decreases after the start of the screening, and the effective radius of the action zone increases strongly in comparison with the radius  $r_f$  of the laser-radiation spot. A possible mechanism of the increase of the zone of action on the target may be thermal defocusing of the laser radiation after passing through the plasma cloud, in addition to absorption of radiation in the plasma; this defocusing lowers the flux density on the target surface.

Estimates made in [8] show that the source intensity should decrease in time like  $\tan^{-1}\sqrt{t}/t_0$  (where  $t_0$  is the time in which the melting temperature is reached on the target surface) in order for the target-surface temperature to change insignificantly during the time from the start of the screening to the end of the pulse. It follows from the experiments, however, that the target-surface temperature decreases with time. This is due to the time variation of the plasma absorption coefficient which lowers the density of the energy flux to the target surface, even though it increases the plasma temperature. The increased distance from the plasmoid to the target also contributes to the lowering of the maximum intensity of the flux on the target surface.

It is interesting to investigate the changes produced in the surface layer of the target material by the joint action of high pressure of the gas and the plasma cloud. Measurements of the microhardness  $H$  of the targets in the radiation zone shows that where there is no melting the microhardness of stainless steel is almost double the initial value (Fig. 5). In the irradiation regions where melting did take place, the microhardness was lower than the initial value.

The change of the microhardness of metallic targets can be connected with two factors: 1) purely structural ones due to the high heating and cooling rates of the material, which lead to the onset of a structure with smaller grain dimensions, introduction of dislocations into the material volume by the thermal stresses, blocking of the existing dislocations, etc., 2) the nitriding of the surface layer, which results in formation of nitrides. At the same time, the melting and the subsequent hardening remove the residual stresses, lead to disordering of the structure, and this naturally lowers the micro-

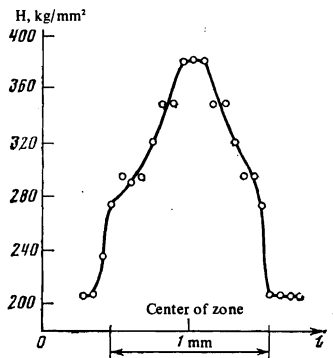


FIG. 5. Distribution of the microhardness in the zone of action of radiation on stainless steel.

hardness of the material. Experiments on saturation of the target material with nitrogen gas show that the average gas content in the beam-action zone increases in comparison with the initial content. As a rule, the nitrogen content is higher than the equilibrium value and increases with increasing nitrogen pressure in the chamber. We note that the analysis of the gas content entails a number of methodological difficulties connected with the smallness of the action zone and the low nitrogen sensitivity of the x-ray spectral apparatus of the "Kameka" type. To analyze the nitrogen content in the action zone we used therefore a spark discharge in an atmosphere of helium at normal pressure.

### 3. DISCUSSION OF RESULTS

In the analysis of the experimental data it is of interest to explain the mechanism whereby the nitrogen breakdown zone develops at low flux density and high pressures, and also to estimate the plasmoid parameters (the absorption coefficient, the temperature, the velocity as functions of the parameters of the experiment).

Let us estimate the threshold radiation flux densities  $q_{thr}$  needed to attain developed evaporation of the target material. In accord with [10,11] we have

$$q_{thr} = \frac{\rho L}{1-R} \sqrt{\frac{a}{\tau}}, \quad (1)$$

where  $\rho L$  is the heat of evaporation per unit volume,  $a$  is the temperature diffusivity coefficient,  $1-R$  is the absorptivity, and  $\tau$  is the time required to reach developed evaporation.

For molybdenum ( $\rho = 10.2$  g/cm<sup>3</sup>,  $L = 6.9 \times 10^3$  J/g,  $a = 0.54$  cm<sup>2</sup> sec) we have  $q_{thr} \approx 1.8 \times 10^6 (1-R)^{-1}$  [W/cm<sup>2</sup>] at  $\tau_p = 0.8$  msec. For polished molybdenum in the temperature range 20–2600°C, in accordance with Svet's data [12] and the recommendations of Dobrovolskiĭ and Uglov [13] that the temperature dependence of the absorptivity be taken into account, it is necessary to assume  $1-R = 0.11$ . Then the threshold of the developed evaporation of molybdenum exceeds  $10^7$  W/cm<sup>2</sup>.

For stainless steel we have  $q_{thr} \approx 3 \times 10^6$  W/cm<sup>2</sup> ( $\rho = 7.8$  g/cm<sup>3</sup>,  $L = 7 \times 10^3$  J/g,  $a = 0.1$  cm<sup>2</sup>/sec,  $1-R = 0.6$ ), i.e., the threshold of the developed evaporation lies inside the range of the flux densities used in the experiments. For dielectrics,  $q_{thr}$  is lower than the laser radiation flux densities employed.

Since most experiments on the metals used by us were performed at flux densities  $q < q_{thr}$ , no developed evaporation was observed during the entire process. This is also confirmed by qualitative pictures of the action of the radiation on a molybdenum target in stainless steel—the outflow of mass was quite small. Calculations also confirm this conclusion.

Let us estimate the growth of the temperature at the center of the heated spot, assuming that the laser radiation intensity has a normal distribution  $q = q_0 \exp(-kr^2)$  over the surface of the target and that the average source power  $P$  does not change during the experiment. Then, for a semi-infinite body (the latter assumption can be made because the time of action is short) the change of the target surface temperature is described by the relation [14]

$$T(0, 0, 0, t) = \frac{P}{\lambda \pi \sqrt{4 \pi a t_0}} \operatorname{arctg} \sqrt{\frac{t}{t_0}}, \quad (2)$$

where  $P = qS$  is the radiation power delivered to the body through the area  $s$ ,  $t_0 = ak/4$ ,  $k = 1/r_f^2$ ,  $\lambda$  is the thermal-conductivity coefficient,  $S = \pi r_f^2$ , and  $r_f$  is the radius of the spot at a level  $1/e$  of the maximum intensity.

The calculated plots of the temperature  $T(0, 0, 0, t)$  on the surface of molybdenum and stainless steel targets are shown for different flux densities in Fig. 6. We see that for  $q \approx 10^6$  W/cm<sup>2</sup> (curve 1) the surface temperature of the target exceeds insignificantly the melting temperature, and for  $t < t_{\text{break}}$  it is less than the boiling temperature at  $p_0 = 1$  atm (the boiling temperature of molybdenum is  $T_b = 4830^\circ\text{C}$ ), the reaching of which can serve as the start of a noticeable development of the evaporation processes. In fact, under the conditions of our experiments ( $p_0 = 1-140$  atm) the boiling point is "shifted" to the region of higher temperatures.

To explain the development of the target-screening plasma cloud in nitrogen at flux densities  $(1-10) \times 10^6$  W/cm<sup>2</sup>, we have considered the following possible mechanism: optical-detonation,<sup>[15]</sup> flash in vapor of the evaporated material,<sup>[16]</sup> slow combustion.<sup>[4]</sup> However, for the action of any of these mechanisms it is necessary to produce an initial ionization zone, which produces in turn the primary absorption of the laser radiation in the gas medium, since the cold gas, at the flux densities  $(1-10) \times 10^6$  W/cm<sup>2</sup> is transparent to the radiation (the flux densities needed for breakdown should be larger by two or three orders than those used above). The primary mechanism of formation of the "priming" plasma can be connected with thermionic electrons, nor can we exclude from consideration the vapor of the evaporated matter or of the oxides that cover the metal, which have a low ionization threshold. The role of the high pressure reduces in this case to containing the electrons for a time  $\sim 0.1$  msec in a region of space on the order of  $\sim r_f^3$  i.e., in the focusing volume.

For molybdenum, the role of the thermionic emission can be the largest inasmuch as in accord with the estimates given above the role of evaporation is small during a time  $\sim 10^{-4}$  sec even at flux densities  $q \sim 10^7$  W/cm<sup>2</sup>.

Ultraviolet radiation from the heated target does not seem to make a noticeable contribution to the breakdown mechanism, owing to the low surface temperature, which exceeds insignificantly (or may even be lower than) the melting temperature. The role of the ionization of the impurities of the gas for the breakdown over the surface of the target is also small, as shown by our experiments without a target.<sup>[7]</sup>

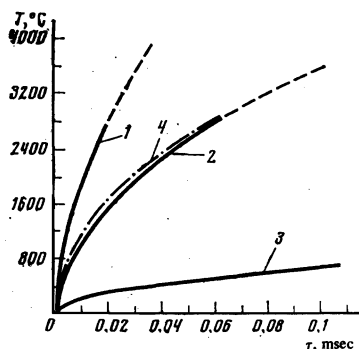


FIG. 6. Calculated time dependences of the temperature on the surface of molybdenum (solid curves; dashed—above the melting point) and stainless steel (dash-dot): 1— $q = 1.1 \times 10^6$  W/cm<sup>2</sup>, 2— $q = 5.5 \times 10^5$  W/cm<sup>2</sup>, 3— $q = 1.1 \times 10^5$  W/cm<sup>2</sup>, 4— $q = 6 \times 10^5$  W/cm<sup>2</sup>.

We have considered in<sup>[8]</sup> the possibility of breakdown plasma formation in nitrogen over a molybdenum target in the case of cascade ionization, when the criterion for the start of breakdown is a definite number of electrons in the volume in which the energy is released. Estimates of the total charge  $e$  (in coulombs) emitted in a time on the order of  $\tau_c \sim 0.1$  msec from an "effective unit area" were made with the aid of the relation

$$e = \frac{r_f^2 \pi B \varphi^2 \tau_c}{k_B^2} \exp\left(-\frac{\varphi \lambda \sqrt{\pi}}{2 k_B q \lambda a \tau_c}\right), \quad (3)$$

where  $B$  is the Richardson constant,  $\varphi$  is the work function, and  $k_B$  is the Boltzmann constant.

The total charge during the time  $\tau_c \approx 0.03$  msec amounts to  $e \sim 10^{-7}$  C, corresponding to  $\sim 10^{12}-10^{13}$  electrons. Comparison with the calculated temperature plot (Fig. 6) shows that the temperature on the surface for  $q \sim 10^7$  W/cm<sup>2</sup> over the target ( $\sim 1.1 \times 10^6$  W/cm<sup>2</sup> on the target) at that instant of time is  $3400^\circ\text{C}$ , which is considerably below the melting temperature ( $T_b = 4830^\circ\text{C}$ ). The accuracy of the temperature calculation depends on how correctly the approximations were made of the time dependence of the pulse, of its spatial inhomogeneity (in comparison with the smooth calculated curve), and of the influence of the temperature dependence of the thermophysical coefficients (the thermal conductivity and the heat capacity) on the temperature field.

An order-of-magnitude estimate of the characteristic time  $\tau_D$  of the diffusion of the electrons from a volume on the order of  $r_f^3$  at a pressure 100 atm can be obtained from the relation

$$\tau_D = r_f^2 / D, \quad (4)$$

where  $D$  is the diffusion coefficient and is equal to  $l_e u_e / 3$ , where  $l_e$  is the electron mean free path and  $u_e$  is the velocity of electrons of energy on the order of the nitrogen ionization energy 14.54 eV. In accordance with (4) we have  $\tau_D \approx 0.06$  msec, which exceeds somewhat the characteristic time of the start of the breakdown  $\tau_{\text{break}} \sim 0.03-0.05$  msec. In estimates based on (4) no account was taken of the electron losses to recombination and formation of negative ions, which apparently can be disregarded at high pressures.

Quantitative estimates of cascade development are difficult since, as noted in<sup>[8]</sup>, as they advance along the energy axis at relatively low flux densities the electrons must cover the nitrogen-atom excitation-energy ranges  $\sim 2$  and  $10$  eV. The presence of excited states hinders the cascade development. On the other hand, if we disregard the excited states hinders the cascade development. On the other hand, if we disregard the excited states, then, in accord with<sup>[17]</sup>, the cascade development time is  $\sim 2 \times 10^{-7}$  sec (at  $q \sim 10^7$  W/cm<sup>2</sup>), which is much less than the experimentally observed breakdown time.

It can therefore be stated that the breakdown mechanism considered by us does not contradict qualitatively the observed phenomena. We note that breakdown due to thermionic electrons should start near the surface, at a distance not larger than  $h = 0.03$  cm.

If the conditions  $q > q_{\text{thr}}$  for developed evaporation are satisfied for the material, then the vapor of the evaporated material can play a role in the development of the primary breakdown zone. In particular, for dielectric vapor the ratio  $\Delta/A$  ( $\Delta$  is the ionization energy of the atom of the vapor and  $A$  is the atomic (or molecular)

weight) can be much less than unity and the condition for the development of an electron cascade, at neodymium-laser intensity, takes the form<sup>[5]</sup>

$$q > 5.6 \cdot 10^9 \Delta/A, \quad (5)$$

where  $q$  is in  $\text{W}/\text{cm}^2$  and  $\Delta$  is in  $\text{eV}$ . Even at  $\Delta/A \approx 0.1$  the threshold flux density greatly exceeds the average value per pulse in our experiments. Thus, breakdown in vapor should occur also in the presence of a sufficient number of electrons, which are supplied to the breakdown zone by thermionic emission. After the absorbing region is produced over the target, the subsequent evolution of the breakdown zone is determined completely by the radiation flux  $q$  and by the gas pressure in the chamber.

The optical-detonation mechanism, which is characterized by supersonic motion of the plasma front,<sup>[15]</sup> is not realized under our conditions because of the low flux densities  $q$ .

A flash in the vapor of the evaporated material<sup>[15]</sup> is not very likely because of the weakly-developed evaporation that precedes the appearance of the breakdown zone, and also because of the essentially non-one-dimensional expansion of the vapor owing to the smallness of the radiation-focusing spot  $r_f$ .

It appears that the motion of the plasmoid in the laser beam direction is realized in our experiments via slow combustion of the beam.<sup>[4]</sup> According to the data of Mul'chenko et al.<sup>[2]</sup> the threshold radiation flux densities needed to maintain the plasma cloud in argon at  $p_0 = 60$  atm were  $q = 15$   $\text{MW}/\text{cm}^2$  and  $P = 20$   $\text{mW}$ . Under our conditions at  $p_0 = 70$ – $100$  atm the plasmoid was maintained at  $q = 10$ – $20$   $\text{MW}/\text{cm}^2$  and  $P = 20$ – $40$   $\text{kW}$  under spiked operation of the neodymium laser, which is close to the data of<sup>[2]</sup>.

Let us estimate the average plasma temperature at the instant of the breakdown and its time variation. In our earlier estimates<sup>[8]</sup> we used the balance equation on the target surface

$$(1 - \alpha d) q + \epsilon \sigma \varphi_{12} T^4 = \frac{2q}{\pi} \text{arccotg} \sqrt{\frac{t}{t_0}}, \quad (6)$$

where  $\alpha$  is the absorption coefficient, which is a function of the plasma temperature,  $d$  is the thickness of the plasma layer,  $\sigma$  is the Stefan-Boltzmann constant,  $\epsilon$  is the integrated degree of blackness, and  $\varphi_{12}$  is an angle coefficient. At constant  $q$ , the right-hand side of (6) decreases, meaning that the absorption coefficient and the temperature of the plasmoid increase. From (6) it follows that the effective screening time, when  $q$  on the target surfaces decreases by one order of magnitude, turns out to be large enough,  $t \sim 10t_0$ .

Substituting in (6) the expression for the absorption coefficient<sup>[17]</sup>

$$\alpha = 6.2 \cdot 10^{-20} n T (h\nu)^{-3} \exp\left(-\frac{\Delta - h\nu}{k_B T}\right) \left[1 - \exp\left(-\frac{h\nu}{k_B T}\right)\right], \quad (7)$$

where  $h\nu = 1.17$   $\text{eV}$ ,  $\Delta = 14.58$   $\text{eV}$  for nitrogen, and  $n$  is the density of the atoms in the plasmoid, which is a function of the temperature, and obtaining numerical estimates for various instants of time, we obtain the dependences of a number of plasma-cloud parameters on the time.

The calculation results are shown in the table. It follows from these data that the temperature and  $\alpha$  increase

Dependence of a number of plasma parameters on the time  $t$  of action of the radiation ( $p = 100$  atm) on molybdenum

Parameter	$q$ , $\text{MW}/\text{cm}^2$	$t$ , sec						
		$5 \cdot 10^{-4}$	$8 \cdot 10^{-4}$	$10^{-4}$	$2 \cdot 10^{-4}$	$3 \cdot 10^{-4}$	$5 \cdot 10^{-4}$	$7 \cdot 10^{-4}$
$T$ , eV	10	1.42	1.463	1.471	1.457	1.465	1.473	1.477
	5	1.35	1.377	1.39	1.417	1.431	1.448	1.456
$\alpha$ , $\text{cm}^{-1}$	10	1.22	1.66	1.71	1.58	1.66	1.73	1.78
	5	0.8	0.96	1.04	1.24	1.35	1.5	1.56
$n \cdot 10^{-19}$ , $\text{cm}^{-3}$	10	4.46	4.33	4.30	4.34	4.32	4.29	4.28
	5	4.69	4.59	4.55	4.46	4.42	4.37	4.34
$v$ , $\text{m}/\text{sec}$	10	11.3	13.4	13.7	13.1	13.6	13.8	14
	5	2.84	3.15	3.28	3.62	3.80	4.02	4.11

monotonically at  $q = 5$   $\text{MW}/\text{cm}^2$ , and then  $\alpha$  and  $T$  oscillate until a steady state is established at  $q = 10$   $\text{MW}/\text{cm}^2$ . The calculated data on the rate of displacement of the plasma cloud as a function of the time, obtained with the aid of relation (8) below, agree satisfactorily with the experimental data (see Fig. 1).

The velocity  $v$  of the plasmoid in the case of slow combustion in the laser beam can be estimated by using the concepts of combustion theory in analogy with<sup>[4]</sup>. We have

$$v = \left[ 2 \frac{\gamma_0(\gamma_0 - 1) a q \alpha(T)}{\gamma(\gamma_0 - 1) \rho_0 C_p T_0 \Delta - h\nu} \frac{k_B T}{\Delta - h\nu} \right]^{1/2}, \quad (8)$$

where the subscript 0 pertains to the cold gas,  $\gamma$  is the adiabatic exponent,  $C_p$  is the heat capacity at constant pressure, and for nitrogen  $\Delta = 14.58$   $\text{eV}$ ,  $h\nu = 1.17$   $\text{eV}$ , and  $a = 40$   $\text{cm}^2/\text{sec}$ . Equation (8) gives the dependence of the plasmoid velocity on the pressure in the form  $v \propto p_0^{-1/2}$ , which agrees qualitatively with the experimental data on the time-dependent section of the action of the pulse. Since the temperature of the plasma increases with time (as does also the absorption coefficient), the plasma velocity increases somewhat during the pulse. This statement agrees with the experimental data (Fig. 1). Equation (8) is valid for estimates only on the time-dependent section of the action of the pulse, inasmuch as the evolution of the plasmoid in the subsequent instants of time is determined by the recombination processes and by the pressure gradient in the direction of the motion. We note that Eq. (8) does not contain any parameters other than the gas constants and the conditions of the experiments (the radiation intensity and its wavelength, the gas pressure).

Let us dwell briefly on the already noted large lifetime of the plasma obtained when radiation acts on dielectrics (bakelite, ceramic). The increase in brightness of the plasma radiation after the end of the pulse can be attributed to release of the energy of the chemical reaction (combustion) of the particles in the plasma. The dimensions of these particles can reach apparently  $10^{-3}$ – $10^{-2}$   $\text{cm}$ . The time required to heat the particles in the plasma to the melting temperature can be estimated from the relation<sup>[18]</sup>

$$\tau_m = \frac{r_0^2}{a K_1^2} \ln \frac{2(T_{\text{plasma}} - T_0)}{T_{\text{plasma}} - T_m} \quad (9)$$

where  $r_0$  is the particle dimension,  $a$  is the temperature diffusivity coefficient,  $K_1 = \sqrt{3Bi}$ ,  $Bi = \alpha_p r_0 / \lambda$ ,  $\alpha_p$  is the coefficient of heat exchange between the particle and the plasma,  $\lambda$  is the coefficient of thermal conductivity of the particle material,  $\alpha_p \sim \lambda_{\text{plasma}} / r_0$ ,<sup>[18]</sup> and  $\lambda_{\text{plasma}}$  is the coefficient of thermal conductivity of the plasma.

Numerical estimates yield  $\tau_m \approx 0.17$  msec for  $r_0$

$= 10^{-3}$  cm and  $\tau_m \approx 17$  msec for  $r_0 = 10^{-2}$  cm, i.e., the time of heating of the particles from the dielectric is long enough and can exceed the pulse duration. If it is assumed that the combustion temperature exceeds the melting temperature (since  $\tau_m$  depends logarithmically on the temperature ratio we have  $\tau_{\text{comb}} > \tau_m$ ), then the obtained estimates do not contradict the observed periodic variation of the plasma temperature after the termination of the radiation pulse.

<sup>1)</sup>These experiments were performed together with S. A. Skotnikov, who developed the procedure for the analysis of the gas saturation.

<sup>1</sup>Yu. P. Raizer, *Usp. Fiz. Nauk* **87**, 29 (1965) [*Sov. Phys. Usp.* **8**, 650 (1966)].

<sup>2</sup>B. F. Mul'chenko, Yu. P. Raizer, and V. A. Épshtein, *Zh. Eksp. Teor. Fiz.* **59**, 1975 (1970) [*Sov. Phys.-JETP* **32**, 1069 (1971)].

<sup>3</sup>A. M. Bonch-Bruevich, L. N. Kaporskiĭ, and A. A. Romanenkov, *Zh. Tekh. Fiz.* **43**, 1746 (1973) [*Sov. Phys. Tech. Phys.* **18**, 1099 (1974)].

<sup>4</sup>F. V. Bunkin, V. I. Konov, A. M. Prokhorov, and V. B. Fedorov, *Pis'ma Zh. Eksp. Teor. Fiz.* **9**, 609 (1969) [*JETP Lett.* **9**, 371 (1969)].

<sup>5</sup>A. I. Barchukov, F. V. Bunkin, V. I. Konov, and A. L. Lyubin, *Zh. Eksp. Teor. Fiz.* **66**, 965 (1974) [*Sov. Phys.-JETP* **39**, 469 (1974)].

<sup>6</sup>V. K. Goncharov, A. N. Loparev, and L. Ya. Min'ko, *Zh. Eksp. Teor. Fiz.* **62**, 2111 (1972) [*Sov. Phys.-JETP* **35**, 1102 (1972)].

<sup>7</sup>N. N. Rykalin, A. A. Uglov, and M. M. Nizametdinov, *Dokl. Akad. Nauk SSSR* **218**, 330 (1974) [*Sov. Phys. Dokl.* **19**, 599 (1975)].

<sup>8</sup>N. N. Rykalin, A. A. Uglov, I. P. Dobrovolskiĭ, and M. M. Nizametdinov, *Kvantovaya elektronika* **1**, 1928 (1974) [*Sov. J. Quantum Electron.* **4**, 1068 (1975)].

<sup>9</sup>I. I. Ashmarin, Yu. A. Bykovskiĭ, N. N. Degtyarenko, V. F. Elesin, A. I. Larkin, and I. P. Sipailo, *Zh. Tekh. Fiz.* **41**, 2369 (1971) [*Sov. Phys. Tech. Phys.* **16**, 1881 (1972)].

<sup>10</sup>S. I. Anisimov, Ya. A. Imas, G. S. Romanov, and Yu. V. Khodyko, *Deĭstvie uzlucheniya bol'shoĭ moshchnosti na metally* (Action of High-Power Radiation on Metals), Nauka 1970.

<sup>11</sup>V. A. Batanov, F. V. Bunkin, A. M. Prokhorov, and V. B. Fedorov, *Zh. Eksp. Teor. Fiz.* **63**, 586 (1972) [*Sov. Phys.-JETP* **36**, 311 (1973)].

<sup>12</sup>D. Ya. Svet, *Vysokotemperaturnoe usluhenie metallov* (High Temperature Radiation of Metals), Metallurgizdat, 1964.

<sup>13</sup>I. P. Dobrovolskiĭ and A. A. Uglov, *Kvantovaya Elektron.* **1**, 1423 (1974) [*Sov. J. Quantum Electron.* **4**, 788 (1974)].

<sup>14</sup>N. N. Rykalin, *Raschety teplovykh protsessov pri svarke* (Calculation of Thermal Processes in Welding), Mashgiz, 1951.

<sup>15</sup>Yu. P. Raizer, *Usp. Fiz. Nauk* **108**, 429 (1972) [*Sov. Phys.-Usp.* **15**, 688 (1973)].

<sup>16</sup>V. I. Bergel'son, A. P. Golub', I. V. Nemchinov, and S. P. Popov, in: *Kvantovaya elektronika* (Quantum Electronics) ed. N. G. Basov **4** (16), Sov. radio, 1973, p. 20.

<sup>17</sup>Ya. B. Zel'dovich and Yu. P. Raizer, *Fizika udarnykh voln i vysokotemperaturnykh gidrodinamicheskikh yavlenii* (Physics of Shock Waves and High-Temperature Hydrodynamic Phenomena), Nauka, 1966.

<sup>18</sup>Yu. N. Lokhov, V. A. Petrunichev, A. A. Uglov, and I. I. Shvyrkova, *Fizika i khimiya obrabotki materialov* (Physics and Chemistry of Metal Working) No. 6, 52 (1974).

Translated by J. G. Adashko

77